Mesoscale Simulations of the November 25-26 and December 5-6 Cirrus Cases using the RAMS Model

J.L. Harrington, Michael P. Meyers, and William R. Cotton

Colorado State University, Dept. of Atmospheric Science, Fort Collins, CO 80523

May 7, 1993

1 Introduction

The Regional Atmospheric Modeling System (RAMS), developed at Colorado State University, was used during the First ISCCP Regional Experiment (FIRE) II (13 November through 6 December, 1991) to provide real time forecasts of cirrus clouds. Forecasts were run once a day, initializing with the 0000 UTC dataset provided by NOAA (Forecast Systems Laboratory (FSL) Mesoscale Analysis and Prediction System (MAPS)). In order to obtain better agreement with obsevations, a second set of simulations were done for the FIRE II cases that occured on 25-26 November and 5-6 December. In this set of simulations a more complex radiation scheme was used, the Chen/Cotton radiation scheme, along with the nucleation of ice occuring at ice supersaturations as opposed to nucleation occuring at water supersaturations that was done in the actual forecast version. The runs using these more complex schemes took longer wall clock time (7-9 hours for the actual forecasts as compared to 12-14 hrs for the runs using the more complex schemes) however, the final results of the simulations were definately improved upon. Comparisons between these two sets of simulations are given in a following section.

Now underway are simulations of these cases using a closed analytical solution for the auto-conversion of ice from a pristine ice class (sizes less than about 50 μm in effective diameter) to a snow class (effective diameters on the order of several hundered μm. This solution is employed along with a new scheme for the nucleation of ice crystals due to Meyers et al (1992) and Demott et al (1993). The scheme is derived assuming complete gamma distributions for both the pristine and snow classes. The time rate of change of the number concentration and mass mixing-ratio of each distribution is found by calculating either the flux of crystals that grow beyond a certain critical diameter by vapor deposition in an ice supersaturated regime or by calculating the flux of crystals that evaporate to sizes below that same critical effective diameter.

2 The Model Description

The purpose of this section is to give a brief description of the set-up of RAMS that was used for the FIRE II experiment. As was mentioned earlier RAMS was initialized with the 0000 UTC MAPS data set because of it's 60 km grid spacing. The set-up of the model included two interactive grids. The first being a course grid of 80 km grid spacing that covered approximately three quarters of the western U.S. The second, fine grid was placed so that it completely covered Kansas and portions of it's boardering states. The fine grid spacing was set to be 20 km. For the vertical resolution, 42 total levels were used with 300m constant spacing up to 9 km. Beyond 9 km the 300 m spacing was slowly stretched until at 16 km the vertical spacing reached 1000 m. For all of the runs, the non-hydrostatic version of RAMS was used with explicit bulk microphysics. Because of the complexity and time considerations, the simulations were done on the National Center for Atmospheric Research's (NCAR'S) CRAY YMP.

3 Comparison of RAMS Forecast Results and Chen/Cotton Radiation Results with Observations

On November 26, 1991 Lidar time height observations (see figure 1) began to pick up cirrus signatures at around 1615 UTC and at a height of about 10km. The cirrus gradually thickend with time; the cloud top remained fairly constant at 10km until around 2024 when it began to vary between values of about 9 and 11 km. The base of the cloud gradually lowered after onset until it reached it lowest point of about 4 km at around 2330 UTC.

Comparing the forecast simulations of the time height profile (Figure 2) with the lidar images shows that the forecast runs were fairly successful in depecting the onset of the cloud and it's basic thickness. The cloud height depicted in the simulation results was a little lower than the 10 km that was observed and the forecast model did not show the low base that the cloud finally achieved. Also, as was noted by Thompson (1993) the mixing ratio values were too small (about one order of magnitude). The simulations that included the more complex radiation scheme (Figure 3) did a noticably better job in the simulation of the time-height cloud profile. Cloud top was at an approximately constant value of 10 km and showed the cloud base lowering; the lowering of the cirrus base was, however, simulated to drop a little below the observed values (about 3.8 km). Another significant improvement was that of larger values of the pristine ice mixing-ratio. Maximum values in the forecast simulation were around 1.8×10^{-6} while the simulations with the Chen/Cotton radiation scheme gave maximums of 0.32×10^{-5}.

Comparison with the satillite image shown in Figure 4 shows that the simulations that included the Chen/Cotton radiation scheme (see Figure 5) predicted the overall placement of the cirrus deck over Kansas very well. The Chen/Cotton scheme has a much lower pristine ice mixing-ratio than the forecast version (not shown), however this is due to the height that the cross-section was taken, maxima in the mixing ratios were as given above.

4 The Auto-Conversion Scheme

As mentionted in the introduction, the auto-conversion scheme is derived assuming that both pristine ice (PI) and snow can be described by complete gamma distributions of the form

$$(1) \qquad n_{pi,s}(D) = \frac{N_t}{\Gamma(\nu)} \frac{D}{D_n} \frac{1}{D_n} exp(\frac{-D}{D_n})$$

where N_t is the total number, ν is the shape parameter, and D_n is the characteristic diameter of the crystal distribution. Using (1) the mass mixing-ratio and total number are defined as:

$$(2) \qquad \bar{r}_{pi,s} = \frac{1}{\rho_a} \int_0^\infty m(D) n_{pi,s}(D,t) dD$$

$$(3) \qquad N_{pi,s}(D,t) = \int_0^\infty n_{pi,s}(D,t) dD$$

where the subscripts pi and s describe the pristine ice and snow distribution respectively. Equations for the flux of vapor onto or away from the total distributions, flux of number and mass from one distribution to another (auto-conversion), and number concentration that evaporates from the PI distribution are derived. Only for vapor depositional growth is considered. The equations for the growth/evaporation of the mass of the complete distributions is calculated by time differentiating (2) above and substituting in the depositional growth equation. For the flux of mass and number, the equations were rewritten in flux form by using the relation

$$(4) \qquad \frac{\partial n(D,t)}{\partial t} = -\frac{\partial}{\partial t}\{I(D,t) n(D,t)\}$$

where I(D,t) is the time derivative of the effective diameter. This relation is then substituted into the time differentiated versions of (2) and (3) above and gives the number and mass of crystals that flux from the PI to the snow distribution during growth conditions or from the snow to the PI distribution during evaporation

conditions. Nucleation of ice crystals is implemented using the emperical relation by Meyers et al (1992) and is given as a simple exponential function of the supersaturation S_i,

$$(5) \qquad NUC = exp\{a + b\{100(S_i - 1)\}\}$$

where a and b are constants used in the emperical fit. The number of crystals that completely evaporates from the PI distribution is found by determining the diameter (D_e) of a particle that will completely evaporate in any given time step. The mass flux of water vapor away from the PI distribution is then broken up into two parts. The first being the mass of PI that completely evaporates and the second term is the amount of mass that is removed from the larger crystals that still remain. Using this method, D_e can then be solved for and the integral of the number concentration up to this D_e can be solved, giving the number of crystals that completely evaporates. An example of the time evolution of the two distributions using this scheme in a simple one-dimensional Lagrangian model is given in Figure 6.

5 Conclusions

RAMS was used to predict the developement of cirrus clouds over Kansas during the FIRE II experiment. The forecast model did a good job of predicting the onset of the November 26 cloud system and also the cloud depth. However, the model had trouble with the cloud top height and the simulation of cloud base. The version of the model that utilized the Chen/Cotton radiation scheme did a better job with these cloud parameters.

Now implemented into a newer version of RAMS is an auto-conversion scheme that allows for the coexistence of small and larger ice crystals. It is expected that this scheme will provide better overall results.

Acknowledgements

Thanks are extended to Greg Thompson for his valuable help with the RAMS model and the FIRE II case study, especially for his help with the Chen/Cotton simulations. Cray Research provided funding (grant # 35081185) for the use of the CRAY YMP during the FIRE II project. This research was supported by the Air Force Office of Scientific Research's grant # AFOSR-91-0296.

References

DeMott, P.J., M.P. Meyers, and W.R. Cotton, 1993: Parameterization and impact of ice initiation processes relevant to numerical model simulations of cirrus clouds. Submitted to *J. Atmos. Sci.*

Meyers, M.P., P.J. DeMott, and W.R. Cotton, 1992: New primary ice nucleation parameterizations in an explicit cloud model. *J. Appl. Met.*, **31**, 708-721.

Thompson, Greogory, 1993: Prototype real-time mesoscale prediction during the 1991-92 winter season and the statistical verification of model data. Masters thesis, Atmos. Sci. Paper No. 521, Colorado State University, Fort Collins, CO, 105pp.

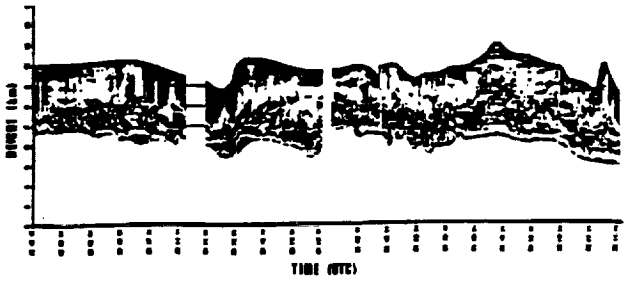

Figure 1: Lidar time-height observations from 1948 UTC to 2214 UTC on November 26, 1991.

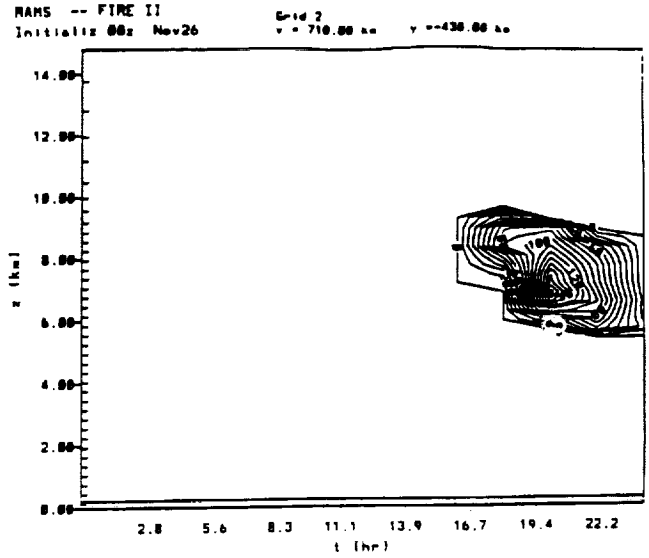

Figure 2: Time-height simulation of the PI mixing-ratio for the actual forecast.

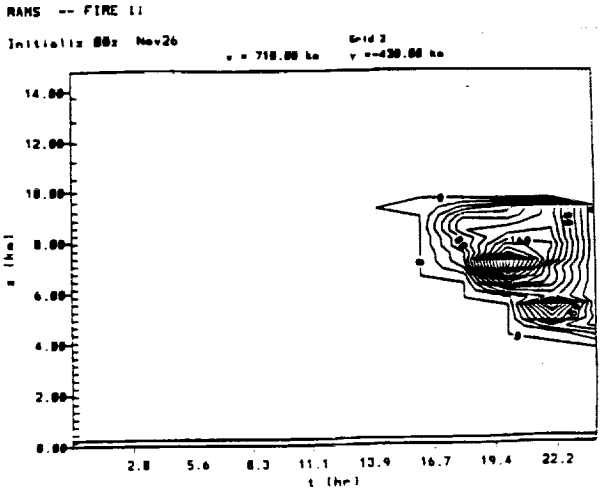

Figure 3: Time-height simulation of the PI mixing-ratio fields for the Chen/Cotton radiation simulations.

Figure 4: Satellite image taken at 1443 UTC on November 26, 1991

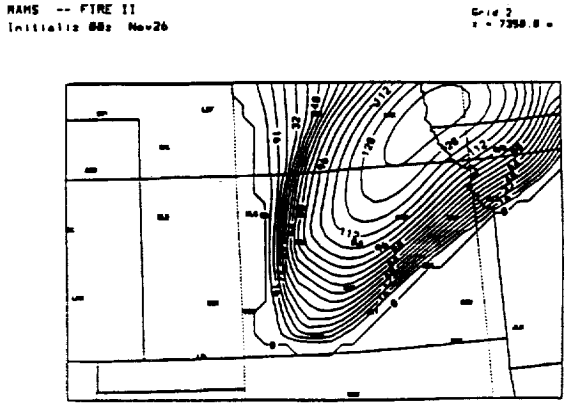

Figure 5: Horizontal cross-section at z = 7350.0 m of the simulated PI mixing-ratio field.

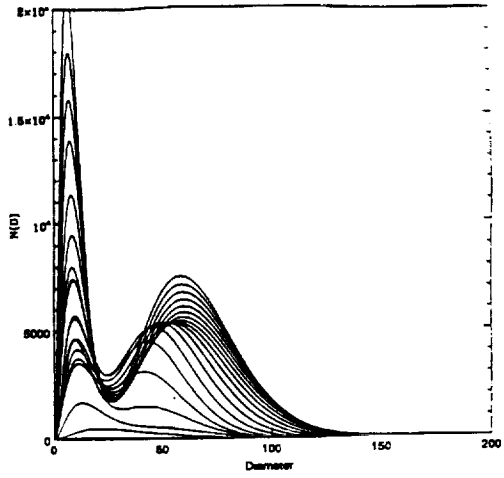

Figure 6: Evolution of the composite gamma distributions for PI and snow